ELSEVIER

Polymer 42 (2001) 6999–7007

polymer

www.elsevier.nl/locate/polymer

The influence of the viscosity ratio on polymer droplet collision in quiescent blends

C. Verdier*

Laboratoire de Rhéologie, Université de Grenoble I, Institut National Polytechnique de Grenoble, CNRS (UMR 5520), 1301 rue de la piscine, BP53-Domaine Universitaire, 38041 Grenoble Cedex 9, France

Received 1 January 2001; accepted 5 March 2001

Abstract

The coalescence of polymer droplets is studied, in particular the final regime named collision. This phenomenon involves the complex deformation of the interface, a motion driven by the interfacial tension, and is mainly governed by the viscosity ratio. An accurate measurement technique of the collision time has been explored experimentally. In a recent paper (Verdier C. C R Acad Sci Paris Série IV 2000;1:119–126), a particular case of the collision was studied, corresponding to viscosities in the same range. One of the aims of the present work is to analyze collision, and to extend these previous results to a wider range of viscosity ratios. For droplets of equal size, three regimes are obtained, corresponding to power law dependence of the collision time as a function of the viscosity ratio.

The flow field shows the importance of the area close to the neck, where most of the flow dissipations occur. By assuming that this flow gives rise to a competition between interfacial energies and shear viscous dissipations, a simple model is presented, based on a previous study (Brochard-Wyart F, de Gennes PG. Advances Colloid and Interface Sci 1992:39:1–11), and it recovers two of the experimental regimes. The final one can also be predicted using results from Frenkel (Frenkel J. J Phys USSR 1945;9:4113–4118). This theory is in qualitative agreement with the observed data.

This experimental technique is simple and provides a new way to measure interfacial tension, when the viscosities of the two fluids are known. The advantage of the technique is that sample preparation is easy, and that it requires only an optical microscope.

Keywords: Coalescence; Droplet; Interfacial tension

1. Introduction

The mixing of two polymers is not quite fully understood, because it requires well-controlled mixers, and the geometry of the blades is generally not simple. Complex flows result from such mixing and it becomes hard to control the size and dispersion of the droplets of one polymer into the other. As mixing goes on, coalescence and break-up of the droplets can happen simultaneously, although they have reasons for appearing, respectively, at low or high shear velocities. In fact, such motions are combinations of both shear and elongational flows, depending on the point in the fluid mixture. Therefore, the application of simple flows is a first step towards the understanding of the mixing process.

Taylor [1] studied well-defined flows such as shear and elongational flows, computed the droplet deformation, and found criteria for break-up. Grace [2] also paid attention to ideal flow situations and studied the critical conditions for break-up and coalescence over a very wide range of viscosity ratios. The break-up problem was again considered in shear and elongational flows using an isolated drop [3,4]. Recently, a few authors [5,6] used microscopy to control droplet size when shearing a polymer emulsion. This situation shows that critical regimes for coalescence [7] and break-up [1] can be established. The latter results are obtained by using a distribution of droplets in a moving fluid, and one assumes a certain probability of encounter for the coalescence process. For example, coalescence requires that a sufficient amount of time (t_e, interaction time) is necessary for the encounter to take place; therefore, an example of such a probability is $P = \exp(-t_d/t_e)$, if t_d is the time necessary to drain the interstitial fluid. If the interaction time is long enough, then coalescence occurs ($P \approx 1$); otherwise, the drainage is not completed ($P \approx 0$). These ideas are reviewed, for example, in Ref. [8].

Let us now consider the ideal situation of a coalescence process with only two droplets. Three parts can be distinguished: the first one is the drainage of the interstitial fluid [8,9], which is very important and controls the total

* Fax: + 33-4-76-82-51-64.
E-mail address: verdier@ujf-grenoble.fr (C. Verdier).

0032-3861/01/$ - see front matter
PII: S0032-3861(01)00183-5

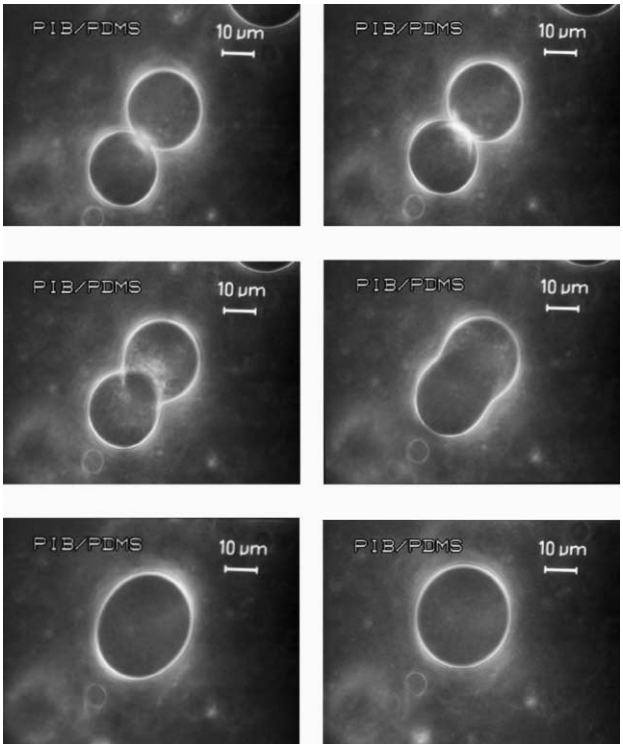

Fig. 1. Collision of droplets of PIB (430 Pa s) in PDMS (60 Pa s): (a) $t = 0$ s; (b) $t = 10$ s; (c) $t = 10.8$ s; (d) $t = 12.4$ s; (e) $t = 16.8$ s; and (f) $t = 21.6$ s.

coalescence time. The second one is related to the opening of a tiny hole which leads to collision. Typically, this process occurs when the gap between the two droplets is smaller than a certain distance (usually about 50 Å), which is probably fluid dependent. The last stage is the collision (or fusion) which corresponds to the merging of the two droplets, which is of interest here, and has not been studied so much in the literature.

This situation has only been considered before in special cases, such as for the flow of crystalline solids under the action of surface tension [10] and in the sintering of metallic powders [11]. A theoretical approach [12,13] based on mapping functions has also been found, but can be applied for the two-dimensional case only. Finally, surface diffusion has also been studied through computations of the initial rapid process [14], showing the initial time dependence. Another recent approach [15] has analyzed the collision process when varying the viscosity ratio of the two fluids, thus showing a dependence of the collision time on the geometric mean $\sqrt{\eta_1 \eta_2}$ of the two viscosities (η_1 for the droplet and η_2 for the matrix). This last work considers the collision as well as the evolution of the neck region, i.e. the point of largest curvature. The viscosity ratio has been varied over two decades, which corresponds to situations where the fluid viscosities are not so different. The fluids used were polymers at small enough rates so that the elasticity effects are negligible. Other studies can be found in the literature concerning the effect of viscoelasticity [16] and the role of copolymers [17] at the interface during coalescence, but are not the purpose here.

In this work, the case of two droplets is considered, bearing in mind the main application, which is the understanding of the dynamics of a polymer emulsion. An overall picture of the role of the viscosity ratio on droplet collision is carried out, with the aim of determining new regimes compared to the previous study [15]. In the first part, the experiment is recalled and new results are presented, over a very large viscosity ratio range (six decades). Three typical regimes are obtained. In the next part, the corresponding theory is proposed, based on the work of Brochard and de Gennes [18]. We also made use of a previous result by Frenkel [10] to explain some of the data. A discussion is proposed next, and the application of this technique as a new interfacial tensiometer is suggested. This technique may be very adequate for the investigation of polymer systems.

2. Experimental part

The experimental system that was used for the observation of collision of the droplets is rather simple and has been presented before [15]. Therefore, we will briefly summarize the method here, as well as the automated technique coupled with it. This technique has been used in order to reduce time consuming data processing. Also, the fluids that were used will be presented. Let us start with the experimental set-up.

2.1. Set-up

An emulsion is first made after mixing two polymers for about 2 min. The mixing can be done manually for example, since the polymer are not too viscous. The system is then set to rest, so that the air entrapped can be released. A small sample is taken from the mixture and put between a plate and a micro cover-glass. Observations are simply made with an optical microscope (Leica, DML model) using a magnification of $\times 20$ or 50, depending on droplet size (usually the radius varies between 5 and 30 μm). One needs to locate two droplets of approximately equal size; therefore, there is a need for a sufficient number of droplets in the blend. This can be easily achieved by mixing enough amounts of polymer 1 inside polymer 2. Once the droplets are located and are close enough, the coalescence process can be visualized. The interstitial fluid 2 is slowly removed (drainage) until the drops actually come very close to each other. Sometimes, a flattening effect is observed, as described previously [8]. Finally a tiny hole is opened, and the collision process takes place. A video camera (3-CCD color, KY-F55B JVC model, 25 frames/s) is coupled to the microscope and films are made on a U-matic videorecorder (SP type, VO-9600P model). Photographs can be downloaded and measurements are made on a PC using the dedicated Labview™ software. A typical experiment is depicted in Fig. 1a–f. Fig. 1a shows two droplets of roughly equal radii getting very close together. In Fig. 1b, the droplets

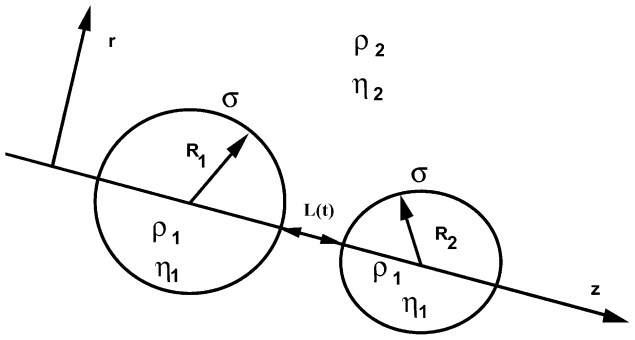

Fig. 2. Schematic picture of the droplets and parameters.

are touching and a hole is opening. After some time (Fig. 1c), the droplets have started to coalesce, until they look like one larger deformed droplet (Fig. 1d). The final stages are next shown while the fluids relax and longer times are needed (Fig. 1e) until the composite droplet finally reaches the shape of a sphere (Fig. 1f).

2.2. System parameters

The system we are looking at (Fig. 2) is an axisymmetric two-droplet system. Two droplets (fluid 1) are imbedded into a matrix (fluid 2). The densities of inner and outer fluid are respectively ρ_1 and ρ_2. Their viscosities are respectively η_1 and η_2. The other parameters of the problem are droplet radii R_1 and R_2 and interfacial tension σ. $L(t)$ is the distance between the droplets, is time dependant and decreases as time goes on. In this case, van der Waals' forces act to bring the droplets close to each other.

To simplify, we will be looking at almost equal sized droplets, so that $R_1 = R_2$. Two such droplets can be found because the system is a dispersion with a large number of droplets. In this problem, a relevant dimensional analysis [15] shows that the only important parameters are the characteristic time of collision t_c (defined more precisely below), in its dimensionless form $\sigma t_c/\eta_1 R_1$, and the viscosity ratio η_1/η_2. Indeed, the Suratman number $S = \sigma\rho_1 R_1/\eta_1^2$ can be neglected because of the high viscosities (>1 Pa s) of the fluids and gravity effects are also negligible in the experiment. Wall effects can also be neglected, by choosing droplets in the center of the fluid (between the plate and micro-cover glass). Let us also note that a typical velocity V is R_1/t_c so that $\sigma t_c/\eta_1 R_1$ can also be interpreted as the inverse of the capillary number. Therefore, we are looking at the dependence of the group $\sigma t_c/\eta_1 R_1$ as a function of the viscosity ratio η_1/η_2. Fluid polymers with various viscosities will be chosen so that a large number of decades can be covered in terms of η_1/η_2.

2.3. Polymers

The fluids are a set of silicones or polydimethylsiloxanes (PDMS, Rhône-Poulenc, 47VT series, viscosities at 25°C: 1, 10, 30, 60, 100, 200 and 1000 Pa s) and polyisobutylenes

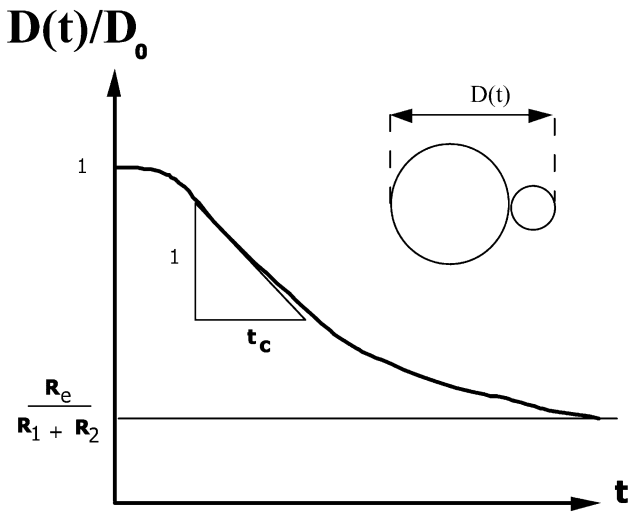

Fig. 3. Typical dimensionless length $D(t)/D_0$ versus time t.

(PIB, D-series, BP-Chimie, viscosities at 25°C: 38, 130 and 430 Pa s). The main advantage of these fluids is that they are melts at room temperature, and they have close enough refraction indexes (1.5 for PDMS and 1.41 for PIB) so that one can observe PDMS in PIB and vice versa. Note that this system has been used by several authors previously [5,6]. It will then be possible to cover a large range of viscosity ratio, basically ranging from 10^{-3} to 10^3, in other words over six decades, which is equivalent to data obtained by Grace [2] for experiments on break-up. These polymers are known to have quite short relaxation times (a few milliseconds) therefore they behave like Newtonian liquids.

2.4. Collision time (t_c)

The characteristic time of collision will be defined as follows. As seen from observations in Fig. 1a–f, the initial starting time of the collision is hard to determine, therefore, we avoid to define a time zero. It is better to plot the total length of the composite droplet $D(t)$ (Fig. 3) and determine the curve $D(t)/D_0$ versus time t, where $D_0 = 2(R_1 + R_2)$. This curve shows an inflexion point at time t_i. The inverse of the negative of the slope, which is homogeneous to a time will be defined as the collision time $t_c = -D_0/D'(t_i)$, where $D'(t)$ is the time derivative of $D(t)$. This is shown in Fig. 3, in the most general case where $R_1 \neq R_2$. One needs to remember that this relation just gives a very precise (mathematical) way to find t_c. Indeed, $D(t)/D_0$ actually ranges between 1 and $R_e/(R_1 + R_2)$, where $R_e^3 = R_1^3 + R_2^3$ from mass conservation. In our case where $R_1 = R_2$, $R_e = 2^{1/3}R_1$. Then $D(t)/D_0$ decreases from 1 to $2^{-2/3} \approx 0.63$. This means that a more realistic coalescence time would be more likely in the range of $0.37t_c$.

This definition is convenient because it is easy to determine t_c experimentally and this definition will be used throughout this paper.

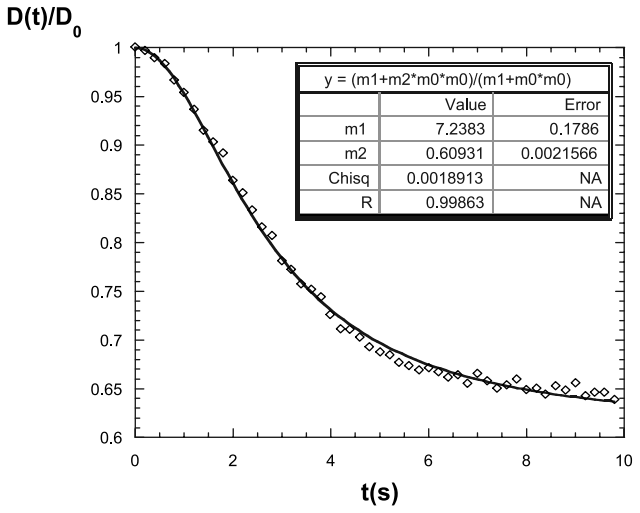

Fig. 4. Experimental curve with equation fit to determine m_1 and m_2 with PIB (130 Pa s) in PDMS (100 Pa s). Best comparison obtained for $m_1 = 7.24\ s^2$ and $m_2 = 0.61$.

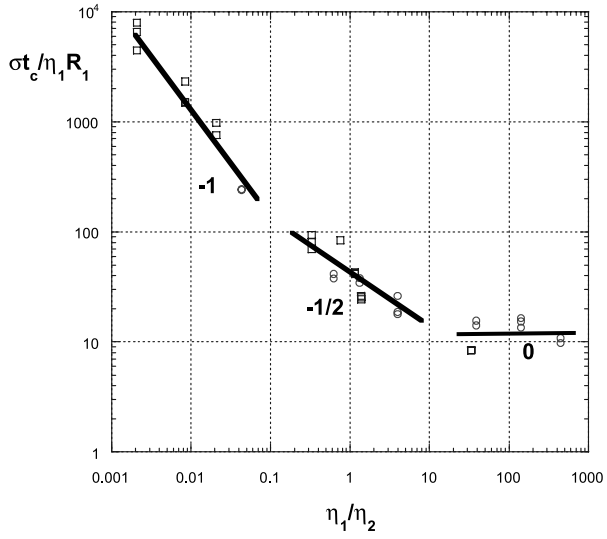

Fig. 5. Dimensionless collision time versus η_1/η_2 ($T = 25°C$).

2.5. Automated determination of t_c

Since a lot of experiments are required in order to cover six decades, we choose an automated system for the measurements and the determination of t_c. Videos are stored on a PC, and the required frames are kept to be analyzed later. Enough data points are chosen so that the rapid decay of $D(t)$ can be monitored accurately. The distance $D(t)$ is measured by pointing a line going through the droplet's axis and the Labview™ software enables to get the distance easily, after a calibration procedure has been used. One can then plot the ratio $D(t)/D_0$ versus time. We choose to fit the data with the following function $F(t) = D(t)/D_0$.

$$F(t) = \frac{m_1 + m_2 t^2}{m_1 + t^2} \tag{1}$$

This function is a good candidate (Fig. 4) because it starts from 1 ($t = 0$), and tends to m_2 ($t \to \infty$). The two parameters m_1 (s^2) and m_2 (dimensionless) can be adjusted using simple fitting tools available on classical graphics software. It is to be checked that m_2 is of the order 0.63 (see previous subsection). It is also found that the curve $F(t)$ is always in good agreement with the experimental data (see Fig. 4).

The other reason for choosing this function is that it shows, of course, an inflexion point, just like in the experiments. After doing some simple algebra, we find that the inflexion time t_i is:

$$t_i = \sqrt{\frac{m_1}{3}} \tag{2}$$

and the slope at the inflection point $F'(t_i) = -1/t_c$ provides the required value of the collision time t_c, once the determination of the two parameters m_1 and m_2 has been made using the automated technique:

$$t_c = \frac{8\sqrt{m_1/3}}{3(1 - m_2)} \tag{3}$$

Fig. 4 shows a set of data, as well as the errors involved in the fitting procedure. The values of the two parameters are found numerically, by optimal fitting. We check that m_1 is positive and that m_2 is close to 0.63, which validates our technique. This systematic determination of the collision time will be used in all the experiments.

2.6. Experimental results

The main results of the experimental part of this work are shown in Fig. 5. The plot of the dimensionless collision time $\sigma t_c/\eta_1 R_1$ as a function of the viscosity ratio η_1/η_2 is given and reveals three different regimes, which correspond to well-defined slopes of -1, -0.5 (roughly) and 0. From the data we can establish three formulae for power-law relationships.

$$0.001 < \eta_1/\eta_2 < 0.1 \qquad \text{slope } -1$$
$$\sigma t_c/\eta_1 R_1 \cong 12(\eta_1/\eta_2)^{-1} \qquad \text{or} \qquad t_c = 12\eta_2 R_1/\sigma \tag{4a}$$

$$0.1 < \eta_1/\eta_2 < 10 \qquad \text{slope } -1/2$$
$$\sigma t_c/\eta_1 R_1 \cong 40(\eta_1/\eta_2)^{-0.5} \qquad \text{or} \qquad t_c = 40(\eta_1\eta_2)^{0.5} R_1/\sigma \tag{4b}$$

$$10 < \eta_1/\eta_2 < 1000 \quad \text{slope } 0 \quad \sigma t_c/\eta_1 R_1 \cong 12(\eta_1/\eta_2)^0$$
$$\text{or} \qquad t_c = 12\eta_1 R_1/\sigma \tag{4c}$$

In these formulae, σ is in N/m, t_c is in s, η_1 is in Pa s and R_1 is in m.

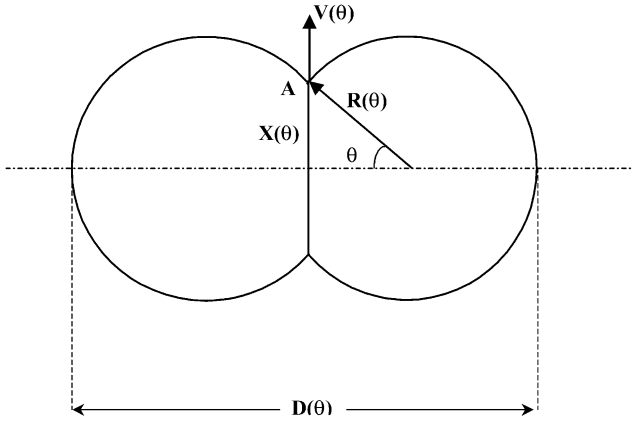

Fig. 6. Geometry of the two-sphere model.

We recover the previous result [15] with the slope of −0.5 which corresponds to a collision time varying as $\sqrt{\eta_1 \eta_2}$, in other words like the geometric mean of the viscosities. Two new regimes are obtained which correspond to collision times varying like the highest viscosity. These regimes seem to be symmetric, because the corresponding constants, equal to approximately 12 (no dimension in formulae (4a) and (4c)) are the same. This result will be discussed in the next sections.

3. Theory

3.1. General framework

Let us look at the geometry of the problem. Two spheres of equal radii collide together and form a new droplet, whose shape can be approximated within good accuracy to the reunion of two spheres (see Fig. 6). We define the angle θ which is convenient for the calculations. θ is a function of time t. From mass conservation, and using the sphere approximation, we can recover the following result due to Frenkel [10], by considering the volume of each part of the spheres: indeed, the fluid density (ρ_1) is assumed to be a constant, therefore, the volume of the new deformed drop is a constant equal to $(8/3)\pi R_1^3$ (the initial volume of both droplets). If $R(\theta)$ is the radius of each of the new spheres (at the beginning of collision), then we find, after some geometry:

$$R(\theta) = R_1\left(\frac{4}{2 + 3\cos\theta - cos^3\theta}\right)^{1/3} \tag{5}$$

Note that $R(\theta)$ is measured from the center of the spheres (Fig. 6), and that this center is moving. Only the center of mass of the spheres is fixed.

The velocity V at the cusp (see Fig. 6) can also be calculated as a function of geometry

$$V = \frac{\dot{}}{R\sin\theta} \tag{6}$$

Formula (6) together with the use of (5) can be combined to obtain the rates $\dot{R}$ and $\dot{\theta}$, after some algebra:

$$\dot{R} = V\frac{\sin^3\theta}{(1 + \cos\theta)^2} \tag{7}$$

$$\dot{\theta} = \frac{V}{R}\frac{2 + 3\cos\theta - \cos^3\theta}{(1 + \cos\theta)^2} \tag{8}$$

Note that V is actually a function of θ: $V = V(\theta)$. It is likely that V starts with a maximum as $\theta = 0$ and decreases as θ increases. Indeed, the driving force (due to interfacial tension) is stronger when the radius of curvature is smaller. We are mainly concerned with the case of small θ, since we are trying to describe the first instants of the collision process, in order to find the characteristic collision time t_c (the steep part of the curve $D(t)/D_0$, see Fig. 3). Other important parameters are the distance $x(\theta)$ and length $D(\theta)$:

$$x(\theta) = R(\theta)\sin(\theta) \tag{9}$$

$$D(\theta) = 2R(\theta)(1 + \cos\theta) \tag{10}$$

Since we are looking at the first stages (rapid) of the collision process, we can make use of the following assumptions, to first order in θ:

$$R(t) \approx R_1 \qquad x \approx R_1\theta \qquad D \approx 4R_1 \qquad \dot{R} \approx V\theta^3/4$$
$$\dot{\theta} \approx V/R_1 \tag{11}$$

This means that the collision time t_c will vary as $\theta_0 R_1/V$, where θ_0 is some angle to be determined. In addition, the rate of change of $D(t)$, designated by $\dot{D}$, can be approximated by

$$\dot{D} = -2V(\theta)\theta \tag{12}$$

From Fig. 3, which provides the collision time definition, we notice that t_c actually corresponds to the maximum slope of $D(t)$ or $D(\theta)$, in other words to the value θ_0 of the angle for which the maximum of the product $V(\theta)\theta$ is obtained. This will be used to predict the typical velocity $V(\theta_0)$.

3.2. Energy balance

The flow involved inside and outside the droplet is rather complex; therefore, we will assume that most of the energy is produced by the driving force, i.e. interfacial tension, and dissipated through viscous flows in both fluids 1 and 2. We will make use of the ideas of de Gennes and Brochard [18,19], who studied the velocity profile inside the corner defined by a plane and an interface with a small angle [18]. Fig. 7 is a good representation of the velocity field. We assume that the angle θ is small. The profile is assumed to be parabolic, due to the lubrication hypothesis in that region of flow. This is valid in this case because, at the beginning of motion, there exists a very small gap between the droplets.

To determine the maximum slope from (12), we need to find the relationship $V(\theta)$. Point A has velocity $V(\theta)$. At point B, there are two components: V_N and V_T are respectively the

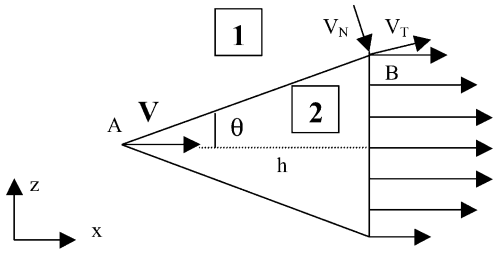

Fig. 7. Sketch of the flow in the neck region.

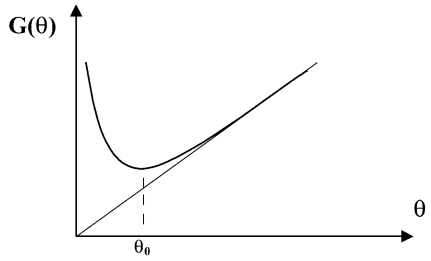

Fig. 8. Function $G(\theta)$.

normal and tangential components (with respect to the interface) of the velocity at B. There are different types of shear which need to be considered, which will lead to dissipation. We approximate V_N by

$$V_N \approx V\theta \tag{13}$$

where θ is considered to be rather small (less than 30° means the error is less that 5%).

V_T can be obtained by writing the continuity of the shear stress at point B, i.e. across the interface: $\eta_1 V_T/h = \eta_2 V/h\theta$, therefore

$$V_T = \frac{\eta_2}{\eta_1}\frac{V}{\theta} \tag{14}$$

Within polymer 1, there are two kinds of shear: $\partial V_z/\partial x \approx V\theta/h$ and $\partial V_x/\partial z \approx V_T/h$.

Within polymer 2, the shear $\partial V_x/\partial z$, from Poiseuille flow, is of the order $V/\theta h$.

From Ref. [18], we write the total dissipation D_v in the system, as the product of the viscosity and the square of the shear rate times the area of concern:

$$D_v = \eta_1\{(V\theta/h)^2h^2 + (V_T/h)^2h^2\} + \eta_2(V/\theta h)^2\theta h^2 \tag{15}$$

It may be remarked that other terms can occur, which are logarithms, but such terms can be considered not to change very much; therefore, they are included in the constants. Anyway, we are only interested by order of magnitudes, and not accurate numbers, due to the approximations already made.

This dissipation is equilibrated by the driving power P, due to interfacial tension, acting in favor of the minimization of the total area. Here, P is given by [19]:

$$P = FV = 2\sigma V\cos\theta \approx 2\sigma V \tag{16}$$

Letting $\epsilon = \eta_1/\eta_2$ we then find:

$$\frac{\sigma}{\eta_1 V(\theta)} \approx \theta^2 + \frac{1}{\epsilon^2\theta^2} + \frac{1}{\epsilon\theta} \tag{17}$$

However, the actual important parameter is $\dot{D}$. After combining Eqs. (12) and (17), $\dot{D}$ is found to be related to θ and ϵ by:

$$\left|\frac{\sigma}{\eta_1\dot{D}}\right| \approx \theta + \frac{1}{\epsilon^2\theta^3} + \frac{1}{\epsilon\theta^2} = G(\theta) \tag{18}$$

where $|A|$ represents the absolute value of A.

Finding the maximum of $|\dot{D}|$ is then equivalent to finding the minimum of Eq. (18), in other words the minimum of $G(\theta)$. The function $G(\theta)$ is first decreasing, then it goes through a minimum at θ_0 until it increases again with an asymptotic behavior $G(\theta) \approx \theta$ (Fig. 8). The minimum is obtained for θ_0 which is the solution of an equation of the fourth order and cannot be simplified. Let us look at the two limiting cases:

Assuming that $\epsilon > 1/\theta_0$, i.e. $\eta_1/\eta_2 > 1/\theta_0$ (neglecting the second term on the right side of (18)), we find that the minimum of (18) is obtained for $\theta_0 \approx \epsilon^{-1/3}$. In this case:

$$\left|\frac{\sigma}{\eta_1\dot{D}}\right| = \epsilon^{-1/3} \qquad \text{and} \qquad V(\theta_0) \approx \frac{\sigma}{\eta_1}\epsilon^{2/3} \tag{19}$$

From the previous section, we found that $t_c \approx \theta_0 R_1/V$ so that $\sigma t_c/\eta_1 R_1$ is equivalent to $\sigma/\eta_1 V(\theta_0)$, so that finally

$$\frac{\sigma t_c}{\eta_1 R_1} \approx \epsilon^{-2/3} \approx \left(\frac{\eta_1}{\eta_2}\right)^{-2/3} \tag{20}$$

This slope is not -0.5, but close to it, and considering experimental errors, it may be concluded that it is in reasonable agreement with the experimental data.

The other case corresponds to $\epsilon < 1/\theta_0$, when neglecting the third term on the right of Eq. (18), i.e. $\eta_1/\eta_2 < 1/\theta_0$ and it is found that the minimum of Eq. (18) is obtained for $\theta_0 \approx \epsilon^{-1/2}$. Then

$$\left|\frac{\sigma}{\eta_1\dot{D}}\right| = \epsilon^{-1/2} \qquad \text{and} \qquad V(\theta_0) \approx \frac{\sigma}{\eta_1}\epsilon \tag{21}$$

In other words

$$\frac{\sigma t_c}{\eta_1 R_1} \approx \epsilon^{-1} \approx \left(\frac{\eta_1}{\eta_2}\right)^{-1} \tag{22}$$

This gives an explanation of the first two slopes (regimes) obtained at very small and moderate viscosity ratios. Since we omitted the constants, it is not possible to determine the exact value of the limiting parameter η_1/η_2 at the change of

regimes, but we may conclude that the order of magnitude is correctly prescribed.

We finally consider the case when the viscosity ratio η_1/η_2 is very large. In this situation, it is difficult to assume a particular type of flow. Therefore, we may recall the solution by Frenkel [10], giving the growth of $x(t)$ when the outer fluid viscosity is small (i.e. η_1/η_2 is very large). In fact this means that we neglect η_2. In this case, $x(t)$ is given by:

$$x^2 = \frac{3R_1\sigma}{2\pi\eta_1}t \tag{23}$$

In addition to Eq. (23), inspection of Fig. 6 leads to this relation for $D(t)$:

$$D(t) = 2R + 2\sqrt{\mathrm{R}^2+\mathrm{x}^2} \tag{24}$$

To first order in θ, we can again assume that $R \approx R_1$. Thus:

$$D(t) = 2R_1\left(1 + \sqrt{1 - \frac{3\sigma\, t}{2R_1\pi\ \eta_1}}\ \right) \tag{25}$$

$F(t)$ now equals $D(t)/4R_1$. It is a decreasing function of time with no inflexion point, but its maximum slope is at $t = 0$, so that $F'(0) = -1/t_c$ (t_c is the point of maximum slope in this case), Therefore, we find a formula for the collision time such that:

$$\frac{\sigma t_c}{\eta R_1} = \frac{8\pi}{3} \approx 8.4 \tag{26}$$

This value has the order of magnitude found previously and is in reasonable agreement with the data (8.4 compared to 12).

A possible improvement of the model is as follows. One needs to consider the exact flow field in the vicinity of the droplets. This will give rise to an exact calculation of the viscous dissipations and the interfacial tension driving power terms. They may actually involve not only shear effects, but the elongational ones as well, because of the complexity of the flow involved. This problem will not be discussed here. It may also be considered numerically. Nevertheless, it can be concluded that this simple model is good enough to be able to predict the three regimes qualitatively, i.e. it is in reasonable agreement with the experiments.

4. Discussion

4.1. Results

The procedure presented in this work is complementary to previous studies which are mostly devoted to studies of the initial phase of coalescence, in other words the drainage problem [8,9]. In particular, Chesters and coworkers have also recently studied numerically the importance of the dispersed to continuous-phase viscosity ratio η_1/η_2 on the drainage problem between interacting drops [20]. They have found limiting cases corresponding to partially mobile or immobile interfaces. The aim of the present work was not to discuss the three stages of the coalescence process, but on the other hand to look at the collision mechanism. As already discussed, the viscosity ratio is the major parameter. It is shown here that limiting regimes are found which are independent of the small viscosity: when η_1/η_2 is small, the time of collision is proportional to η_2, the large viscosity. Similarly, when η_1/η_2 is large, t_c is proportional to η_1, the large viscosity. From the experiments, the relation is given approximately by $t_c \cong 12\eta R_1/\sigma$ (where η is the large viscosity). Interestingly, the constant is the same in both cases, although there is no symmetry here. The first case is the one where one pushes a very viscous fluid, whereas the second one is related to motion of a very viscous fluid pushing a much less viscous one. Locally, at the neck, the velocity field is dominated by the interface velocities and all the dissipation comes from a very small region close to the apparent cusp. Therefore, we may explain this result by assuming that the local flow is the same in both cases, and that it controls the local dissipation. This is also the reason why the model of de Gennes and Brochard [18,19] is used here, for it assumes that the dissipation occurs only in a very small region close to the singular point. Most likely, the flow in such situations is close to a plug flow. Another interesting study would be to determine the exact shape of the velocity profile.

The problem of the singular point is also of concern, because one may argue that Figs. 6 and 7 are drawn as if there was a cusp. One may also refer to other similar works where cusps are discussed, such as when pulling a fluid with a cylinder, half immersed in this fluid [21,22]. Indeed, Newtonian and non-Newtonian fluids are considered to allow this type of situation, going from a cusp to a gradually smooth curvature. In particular, asymptotic analyses can allow one to treat such problems, and also allow the effect of interfacial tension. In our case, we consider that the shape of the free surface at the moving boundary point A is initially a cusp, but after a very small time, it certainly corresponds to a small (compared to R_1), but finite radius of curvature. This can also be observed from Fig. 1a–f. Probably, another important problem would be the close experimental analysis of the so-called cusp, especially at very small times.

Speaking about the theoretical part leads us to pose the question of the intermediate slope which is predicted by a power law of $-2/3$ instead of -0.5 experimentally. Nevertheless, it is likely that changing fluid 1 into 2 should not give the same result, except in the limiting cases where one viscosity is dominant. Generally speaking, the slope of $-2/3$ may seem quite reasonable. The errors on data points can allow one to think that a slope of $-2/3$ agrees well also with experimental points. Errors may be due to the fact that only approximately equal spheres are considered here, and that the influence of the ratio of the radii R_1/R_2 can affect some of the measurements.

4.2. Perspectives

This work leads to the natural improvement of this technique into an interfacial tensiometer for polymers. Such apparatuses are well known to physicists and are of different types. The most common ones available nowadays are based on the filament break-up technique [23], or the retraction of an ellipsoid [24], whereas the spinning drop tensiometer [25,26] or the usual pendant-drop technique [27] are older techniques but still give valuable information. The technique proposed here can be used as a measuring device as well. It requires only a microscope, which is available in most research laboratories or private research centers. The mixing of the fluids is quite easy and the only needed parameters are the viscosities at the required temperature. The only quantity to be measured is the collision time. This is probably better achieved using a video camera with a well-defined speed (frames/second). In the experiment, 40 ms (1/25 s) was the fastest time interval between the frames and it was fast enough for such fluids. It should also be perfectly adapted for highly viscous fluids, such as molten polymers.

One the major advantages of the technique is that sample preparation is quite easy, and mixing of the fluids is easily achieved using small amounts. This is much better than in other techniques such as the filament break-up, for example, which requires the molding of a long regular filament inside another polymer. The amount of time required for the experiments is, of course, viscosity dependent and may turn out to be long, but one may use higher amounts of fluid 1, in order to obtain many droplets. In such a system, one can then pick two very close droplets. Thus, we limit the time to drain fluid 2, since the initial conditions correspond to small gaps or films. Once the collision process has started, it is only required to capture the first instants, as described, and this method has the advantage of being time-saving. It is not needed to wait until final relaxation.

Temperature control may be one problem, if one wants to study (under a microscope) polymers which are in their molten state at high temperatures. Up to now, the author is only aware of heating systems to be operated with a microscope up to 100°C. On the other hand, it is possible to design heating systems (up to 250°C) to be operated under other visualization systems. The use of a macro lens coupled with a high resolution camera (1/3″ size) can constitute an interesting solution.

The final question is also to relate the collision time with the interfacial tension. The answer is given by formulae (4a)– (4c). Depending on the viscosities of the fluids, one will have to use one formula, or another. This may be an advantage, because the use of low viscosity fluids is convenient. Indeed, they are easier to handle and the corresponding collision times are shorter. Still, one has to be careful about the molecular weight dependence of interfacial tension in polymeric systems, which may affect the results [27].

Another interesting aspect will be the study of the influence of the viscoelastic properties of the polymers on droplet collision. This has been introduced by a few authors [16] and an interesting comparison may be drawn. Finally, the influence of copolymers (type, triblock or diblock, architecture, length, etc.) at the interface is also another possible application for such a tensiometer.

5. Conclusion

In this work, a simple experiment on droplet collision is presented. The effect of the viscosity ratio on the collision time has been considered with a wide range of fluids, covering about six decades of viscosity ratio. Three different regimes have been found experimentally. If the viscosity of one fluid (droplet or matrix) is much larger, then it governs collision. In the other intermediate case (viscosities in the same range), then the collision time varies approximately as the geometric mean of the viscosities, as observed previously.

Due to the very rapid growth of the neck, we have proposed a model considering the local viscous dissipations at the neck. This model gives a qualitative description of the viscosity ratio influence on the collision time.

Finally, an extension of this method to the design of a new interfacial tensiometer has been proposed, and its application for melts is possible. The influence of viscoelasticity and/or the influence of compatibilizers at the interface may also be interesting problems to consider with this technique.

Acknowledgements

The author is grateful to P.G. de Gennes and F. Brochard-Wyart for their helpful suggestions concerning the theoretical part.

References

[1] Taylor GI. Proc Royal Soc 1879;29:501–23.
[2] Grace HP. Chem Eng Commun 1982;14:225–77.
[3] Barthès-Biesel D, Acrivos A. J Fluid Mech 1973;61:1–21.
[4] Acrivos A, Lo TS. J Fluid Mech 1978;86:641–72.
[5] Grizzuti N, Bifulco O. Rheol Acta 1997;36:406–15.
[6] Vinckier I, Moldenaers P, Terracciano AM, Grizzuti N. AIChE J 1998;44:951–8.
[7] Janssen JMH. Dynamics of liquid-liquid mixing. PhD thesis. Eindhoven University of Technology. Eindhoven. The Netherlands, 1993.
[8] Chesters AK. Trans I Chem E 1991;69A:259–70.
[9] Fortelny I, Zivny A. Polymer 1995;36:4113–8.
[10] Frenkel J. Phys USSR 1945;9:385–91.
[11] Kuczynski GC. Transactions AIME 1949;185:169–78.
[12] Hopper RW. J Fluid Mech 1990;213:349–75.
[13] Hopper RW. J Fluid Mech 1992;243:171–81.
[14] Eggers. J Phys Rev Letters 1998;80:2634–7.
[15] Verdier C. C R Acad Sci Paris Série IV 2000;1:119–26.
[16] Mazur S, Plazek DJ. Prog Organic Coat 1994;24:225–36.
[17] Sundararaj U, Macosko CW. Macromolecules 1995;28:2647–57.
[18] Brochard-Wyart F, de Gennes PG. Advances Colloid Interface Sci 1992;39:1–11.

[19] de Gennes PG, Brochard-Wyart F. 2000, unpublished result.
[20] Bazhlekov IB, Chesters AK, van de Vosse FN. Int J Multiphase Flow 2000;26:445–66.
[21] Joseph DD, Nelson J, Renardy M, Renardy Y. J Fluid Mech 1991;223:383–409.
[22] Joseph DD. J Non Newtonian Fluid Mech 1992;44:127–48.
[23] Cohen A, Carriere CJ. Rheol Acta 1989;28:223–32.
[24] Luciani A, Champagne MF, Utracki LA. J Polym Sc B: Polym Phys 1997;35:1393–403.
[25] Elmendorp JJ, de Vos G. Polym Eng Sci 1986;26(6):415–7.
[26] Joseph DD, Arney MA, Gillberg G, Hu H, Hultman D, Verdier C, Vinagre TM. J Rheol 1992;36(4):621–62.
[27] Wu S. Polymer interface and adhesion. New York: Marcel Dekker, 1982.